



# Development and Evaluation of Mouth Dissolving Nanofibers for ampicillin

**Kavish Bansal<sup>1</sup>, Monika Bansal<sup>2</sup>, Babaldeep Kaur<sup>3</sup>, Jasleen Kaur<sup>4</sup>**

Akal College of Pharmacy & Technical Education, Mastuana Sahib, Sangrur, India – 148 001

Corresponding author:

Mrs. Monika Bansal; Associate Professor

E mail: monikabansal8@gmail.com

## ABSTRACT:

The present study successfully fabricated mouth dissolving nanofibrous loaded with Ampicillin using PVP K90 as the polymer matrix and ethanol as the solvent to enable efficient electrospinning and ensure proper fiber formation. The nanofibers demonstrated favorable pharmaceutical characteristics, including appropriate thickness, mechanical strength, rapid disintegration, and efficient drug loading. The SEM analysis confirmed the formation of uniform nanofibers, and the dissolution studies revealed that the films provided a controlled and sustained release of the antibiotic at the site of infection. This formulation has the potential to offer significant therapeutic advantages over conventional antibiotic treatments for local throat pathologies, including faster onset of action, localized drug delivery, and reduced systemic side effects. By minimizing the dosage required and targeting the infection site more effectively, this nanofibrous film can contribute to better patient compliance and outcomes.

## Introduction:

### *Nano-fibres:*

Nanofiber technology is an exciting area attracting the attention of many researchers as a potential solution to the current challenges in the biomedical field such as burn and wound care, organ repair, and treatment for osteoporosis and various diseases. Nanofibers are attractive in this field for several reasons. First, surface area on nanofibers is much higher compared to bulk materials, which allows for enhanced adhesion of cells, proteins, and drugs. Second, nanofibers can be fabricated into sophisticated macro-scale structures (Nadaf, Gupta et al. 2022). The ability to fabricate nanofibers allows renewed efforts in developing hierarchical structures that mimic those in animals and human. On top of that, a wide range of polymers can be fabricated into nanofibers to suit different applications. Nanofibers are most commonly fabricated through electrospinning, which is a low-cost method that allows control over fiber morphology and is capable of being scaled-up for mass production (Jayaraman, Kotaki et al. 2004).

Nanofibers are nanostructures with dimensions in the range of nanometer scale (1 to 100 nm). These structures are one dimensional (1D), with a diameter of less than 100 nm. A variety of polymers were reduced to nanofibers with diameters ranging from 50 to 100 nm. Because of their special qualities, industries and researchers are interested in using nanofibers for a variety of purposes. Smaller pore size, high porosity, high aspect ratio, large specific area, ability to retain electrostatic charge, and excellent pore interconnectivity are just a few of the benefits that come with scaling down microfibers to nanometers (Yang, Du et al. 2022). All polymer nanofibers are distinct due to their large surface area to volume ratio, high porosity, noticeable mechanical strength, and flexibility in functionalization. Nanofibers can be synthesized via a variety of techniques, including electrospinning, self-assembly, phase separation, drawing, and template synthesis. Among them, electrospinning is a straightforward, inexpensive, and highly productive method that makes it simple to produce nanofibers of various sizes (Li, Xiao et al. 2022) (Yoon, Hsiao et al. 2008).

## Materials and methods:

### 4.3.1. Preformulation Studies

#### 4.3.1.1. Organoleptic Properties

Organoleptic evaluation of ampicillin trihydrate was performed by visual observation of visual viz parameters like colour, appearance, and other physical characteristics.

#### 4.3.1.2. Melting Point

A Capillary melting point apparatus was used by filling in one sided sealed capillary to determine the melting point of the drug (Dorofeev, Arzamastsev et al. 2004).

#### 4.3.1.3. Solubility

The solubility of ampicillin trihydrate was studied in various solvents like ethanol, methanol, DMSO, DMF and distilled water. An excess amount of the drug was suspended in 5 mL of different solvents at room temperature in an airtight container or conical flask and shaken on a wrist action shaker for 24 hr. The solubility determined was expressed as parts of solute dissolved in parts of solvent (Savjani, Gajjar et al. 2012)

#### 4.3.1.4.

##### Spectroscopic Studies:

UV - Visible Spectrophotometry has been used as a tool for identification of various drugs to obtain specific information related to chromatographic part of the molecule. Organic molecule in solution when exposed to light depending on the type of electronic spectrum absorb light of particular wavelength depending on the type of electronic transition with the associated with the absorption (Sension, Chung et al. 2022).

##### • Absorption Maxima ( $\lambda_{max}$ )

Ampicillin Trihydrate solution (10  $\mu$ g/ml) in water was taken in Cuvette and scanned in the range of 200–400nm on a UV- Spectrophotometer (Shimadzu, Japan) against respective blanks in the range of 1–10  $\mu$ g/ml following by these steps.

- 1) 10 mg of ampicillin trihydrate was dissolved in 10 mL of water in a test tube, which was referred to as Stock A.
- 2) 29.7 mL of water was taken in another test tube, and 0.3 mL from Stock A was added, forming Stock B.
- 3) The number of dilution steps was calculated based on the concentrations of Stock A and Stock B.
- 4) Stock B was used for UV determination, and its  $\lambda$ -max was observed at 228 nm with an absorbance of 0.063.

A standard plot was created using the scatter equation ( $Y = 0.0279X - 0.0131$ ,  $R^2 = 0.9983$ , S.D = 4.45%,  $N = 7$ ,  $p < 0.0001$ ), where Y represented the peak height at 228 nm, and X represented the concentration in mg/L.

##### Standard Curve of ampicillin trihydrate in Water

Ampicillin trihydrate (10 mg) was dissolved in 10 mL of water to prepare Stock A, which was further diluted tenfold to obtain Stock B. Stock B was scanned under a UV spectrophotometer at 228 nm to determine absorbance. A 30 mL solution of Stock B (10  $\mu$ g/mL) was prepared, and various aliquots of concentrations ranging from 5 to 30  $\mu$ g/mL were obtained. A calibration curve was plotted using absorbance (y-axis) and concentration (x-axis), yielding a linearly regressed relationship.

Partition coefficient of excess drug was determined by using shake flask method with water and n-octanol. 50 mg of ampicillin trihydrate acetate was taken in a conical flask to which 20 mL of water and n-octanol was added in the ratio of 1:1 and then placed upon rotary shaker for 24 h. The mixture was then transferred to a separating funnel and was allowed to stand for 30 min (Kato, Hagihara et al. 2022).

$$(k_D)A = \frac{[A]_{org}}{[A]_{aq}}$$

where  $K_D$  is the process equilibrium constant represents the concentration of solute  $[A]_{aq}$  being tested, and "org" and "aq" refer to the organic and aqueous phases respectively (Walczak, Iwaszkiewicz-Grześ et al. 2024).

#### 4.3.1.6 Fourier Transformation Infrared Spectroscopy

Ampicillin trihydrate's functional groups (amino, carboxyl and carbonyl) were identified by FTIR spectroscopy which detects molecular vibrations and is sensitive to structure and environment. This method is effective for studying biomolecules and biochemical changes in tissues. For FTIR analysis, powder samples were prepared by evaporating water uses a hot stirrer and measured 600–4000  $\text{cm}^{-1}$  range at room temperature (Kida, Konopka et al. 2023).

#### Formulation Development

##### Electrospinning Machine Process Parameters

- Flow Rate: 1.5 mL/hr
- Distance: 12 cm
- Voltage: 20Kv
- Syringe Type: 2.5mL
- Needle Diameter: 4.2mm

##### Other Parameters

- Each solution was stirred on magnetic stirrer for ~20–30 min
- The as-spun nanofibers were left to dry overnight

#### 4.4.2 Instruments Details

Developed electrospinning setup, Super ES-3 (E-Spin Nanotech Pvt Ltd, India)

**The technical specification of Electrospinning machine is as follows (Cui, Zheng et al. 2018):**

- Have high voltage supply up to 30Kv.
- User interface for setting up feed rate, drum speed, applied voltage.
- Provides option for 2ml to 5ml syringes for the solution.
- Comes with rotating drum, thus producing continuous nanofibers.
- Plastic enclosed to avoid dust and provide vacuum environment.
- Can produce nanofibers in micro and nanometre scale.

#### Preparation of ampicillin trihydrate loaded Nanofibrous Oro-dispersible Film by Electrospinning Method

##### Materials system

Ampicillin trihydrate, Polyvinylpyrrolidone K90 (PVP k90) (MW = 360000 g/mol), Citric acid (MW = 192.124 g/mol) and Ethanol (MW = 46.07 g/mol).

##### Preparation of ampicillin trihydrate loaded Nanofibers by electrospinning

Anhydrous ethanol, a 'class 3'FDA-approved solvent, was chosen for electrospinning due to its rapid evaporation and ampicillin trihydrate solubility. To prepare the solution, 2% citric acid was mixed with 40 ml ethanol, followed by the addition of the drug and 15% PVP K90. The mixture was sonicated for 30 minutes to ensure homogeneity. Optimizing parameters, electrospinning was performed for 3 hours to obtain the nanofibers mat.

##### Screening of Orodispersible polymers

For the screening of the polymers for the final formulation four polymers were selected and the electrospinning process was applied on the different combination of polymers at variable concentrations electrospinning process was applied on the different combination of polymers at variable concentrations (Edmans, Clitherow, et al., 2020 (Azari, Golchin et al. 2022; Ahmadi Bonakdar and Rodrigue 2024). The selected polymers with different concentrations are depicted in the Table 4.3:

**Table 4.3: Screening of polymers for the final formulation**

S.No	Polymer A	Conc. A	Polymer B	Conc. B	Solvents
E1	Sodium alginate	2.5%	PVA	10%	Water
E2	PVA	5%	PVP K30	5%	Water
E3	PVP K90	20%	-	-	Ethanol
E4	PVP K90	20%	CMC	1%	Ethanol water
E5	PVA	10%	PVP K90	20%	Water
E6	PVA	10%	PVP K90	10%	Water
E7	PVA	7%	PVP K90	7%	Water
E8	PVP K30	20%	-	-	Water

#### Characterization of Optimized Drug Loaded Nanofibrous Oro-dispersible film

##### Visual appearance

Visual inspection of the prepared nanofiber film was done to identify the physical form and uniformity of polymeric blend in the prepared formulation. The prepared film was evaluated for its physical appearance, texture and uniformity in all directions (Abd Razak, Wahab et al. 2015)

##### 4.4.5.2 Thickness of the fiber mat

A 2×2 cm<sup>2</sup> sections of nanofibrous mat was cut out then the thickness of each section was measured by using a digital Vernier caliper (Sharma, Thakur et al. 2014)

### Folding endurance

The folding endurance gives a measure of the brittleness of a film. A 2×2 cm<sup>2</sup> section of mat were repeatedly folded by hand at the same line until they broke or a visible crack was observed. The number of times a film can be folded without breaking or visibly cracking is defined as the folding endurance (Ryu, Koo et al. 2020).

### pH of the fiber solution

A 2×2 cm<sup>2</sup> section from formulation was dissolved in 10 mL of distilled water and the pH was measured using pH meter (IGene Labserve, New Delhi, India). This experiment was carried out in triplicate (Hoseyni, Jafari et al. 2020; Al-Shaeli, Benkhaya et al. 2024).

### Morphology

The fiber morphologies were assessed using a scanning electron microscope (ZEISS LEO 435 VP, Zeiss, Germany). Prior to examination, the samples were gold sputter-coated under argon to render them electrically conductive. Images were then recorded at an excitation voltage of 20 kV. The average fiber size was determined by measuring their diameters at over 50 points in SEM images, using the Zeiss Zen software. Six images were analyzed at different magnification ranges from 500X to 10 kX (Zaarour, Zhu et al. 2020).

### Tensile strength

Tensile strength of nanofibers was measured using a texture analyzer (TAXT plus, Stable Micro Systems, UK) by applying 5 kg load cell equipped with tensile grip holder. The sample was cut into square shape with dimensions of 20 x 20 mm<sup>2</sup>. The texture analyzer was allowed to run with a sensitivity force of 3 gm/cm<sup>2</sup>. and the force required to break or split the nanofiber into two pieces was determined (Pérez-González, Villarreal-Gómez et al. 2019).

### Rheology of polymeric solution

The viscosity of polymeric solution was measured using an MCR 102e rheometer (Anton Paar, Graz, Austria) with a plate-plate measuring system PP25 (25 mm diameter) at a constant temperature (25 ± 0.1 °C) and with a sample volume of approximately 0.9 mL. Shear rate sweep tests were performed with 21 points in the range of 0.1 to 100 s<sup>-1</sup> (Bayer 2021).

### Fourier transform infrared spectroscopy

FTIR analysis of nanofibrous orodispersible films involved preparing a clean sample section, calibrating the instrument with a blank background spectrum, and scanning the film over 4000–400 cm<sup>-1</sup>. The recorded spectra were analyzed to identify peaks corresponding to functional groups, revealing chemical composition and interactions. Results were compared with reference spectra to confirm key compounds or detect impurities (Colley et al., 2018a).

### Disintegration

3 cm diameter circular sections were cut from the fiber mats using a biopsy cutter and placed in a Petri dish containing 15 mL of simulated saliva (NaCl 8.00 g, KH<sub>2</sub>PO<sub>4</sub> 0.19 g, Na<sub>2</sub>HPO<sub>4</sub> 2.38 g, in 1 L of distilled water; pH 6.8) at room temperature. The disintegration and dissolution of the fiber mats was recorded at using a high speed video camera (Tort & Acartürk, 2016b).

### Dissolution studies

The standard British Pharmacopoeia dissolution test is performed in 900 mL of a dissolution medium. However, this does not reflect the volume of the oral cavity. Therefore, a modified dissolution study was performed using a 1 cm long magnetic stirrer in a 7 cm diameter glass Petri dish. 15 mL of simulated saliva pre-warmed to 37°C was placed in the Petri dish and stirred at 150 rpm on a multipoint stirrer. 200 µL of the sample was removed at pre-determined time points and replaced with 200 µL of pre-warmed simulated saliva to maintain a constant volume. Experiments were carried out in triplicate. The temperature remained at 37± 2 °C throughout the experiment (Singh et al., 2016).

### Drug Loading and Entrapment Efficiency:

To determine the loading of Ampicillin Trihydrate within the fibers, approximately 5 mg of loaded electrospun nanofibers were dissolved in 5 mL of water to fully dissolve the drug and polymer. The obtained solution was analyzed using UV visible spectrophotometer (Shimadzu, Japan). The reading was compared against the calibration curve obtained using standard samples of 5-30 µg/mL of ampicillin in water. The absorbances at 228 nm were recorded and the experimental ampicillin loading (%) in the nanofibers was calculated by using the formula:

$$\text{Drug loading (\%)} = \frac{M_d}{M_p} \times 100$$

Where,  $M_d$  is the mass of the drug obtained experimentally as described above and  $M_p$  is the total mass of the analyzed sample (Singh et al., 2016).

- **Entrapment Efficiency:**

Entrapment efficiency refers to the percentage of the active drug successfully encapsulated or retained within the film matrix compared to the initial amount used in the formulation. It is calculated using the formula:

$$\text{Entrapment Efficiency (\%)} = \frac{\text{Amount of drug in film}}{\text{Initial amount of drug use}} \times 100$$

### Weight variation

The assessment of weight variation is performed by weighing individually five films of every formulation on a digital balance. The average weight is calculated and the standard deviation from the average weight is measured.

## 5.RESULTS AND DISCUSSION

### Preformulation Studies

#### Organoleptic Properties

Organoleptic properties of ampicillin trihydrate are shown in Table 5.1

**Table 5.1: Organoleptic properties of ampicillin trihydrate**

Sr. No.	Parameter	Observation
1	Colour	Yellowish
2	Physical Appearance	Solid

#### Melting Point

Melting point of ampicillin trihydrate was found to be 194°C. The melting point reflects the temperature at which ampicillin trihydrate transitions from a solid to a liquid state, which is important for its formulation and stability in pharmaceutical applications.

#### Solubility

Solubility of ampicillin trihydrate was determined in different solvents including distilled water, ethanol, DMSO, DMF and methanol. The solubility of ampicillin trihydrate revealed that it is soluble in methanol, ethanol, DMSO and DMF. It was practically insoluble in chloroform, ether and benzene as shown in (Table 5.2).

**Table 5.2: Solubility of ampicillin trihydrate**

Solvent	Observed Value
Methanol	7.5mg/ml
Water	0.958mg/ml
Ethanol	3.4mg/ml
DMF	5mg/ml
DMSO	25mg/ml

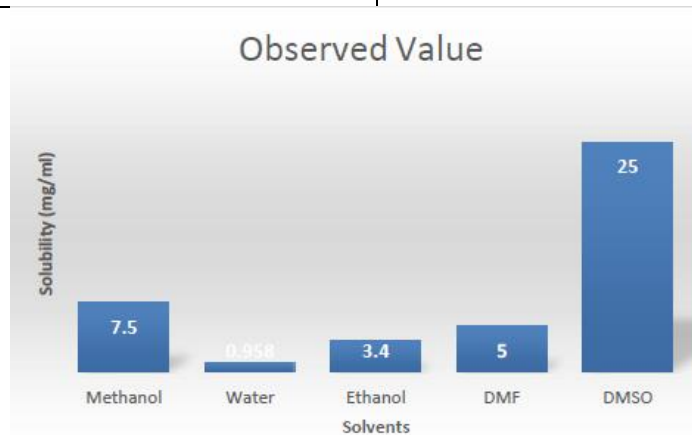


**Figure 5.1: Solubility data of ampicillin trihydrate in different solvents**

### Partition Coefficient

Partition coefficient of drug was found to be -0.24. Solubility of ampicillin trihydrate in both oil and water phase was determined by calculating partition coefficient using shake flask method with water and n-octanol. 10 mg equivalent of ampicillin trihydrate were taken in a conical flask to which 10 ml of water and n-octanol was added and then placed upon rotary shaker for 24 h. The mixture was then transferred to a separating funnel and was allowed to stand for 30 min. Partition coefficient of ampicillin trihydrate can be calculated by using the formula:

$$(KD)_A = [A]_{org}/[A]_{aq}$$

where  $KD$  is the process equilibrium constant,  $[A]_{org}$  represents the concentration of solute  $[A]_{aq}$  being tested, and "org" and "aq" refer to the organic and aqueous phases respectively (Toehwéet al., 2017).

### Fourier transform infrared (FTIR) spectroscopy

FTIR was performed on ampicillin trihydrate, PVP K90 and citric acid in which all the principal functional peak as well as other characteristic peaks were observed. The FTIR graph of drug depicted in (Figure 5.2) and (Table 5.3).

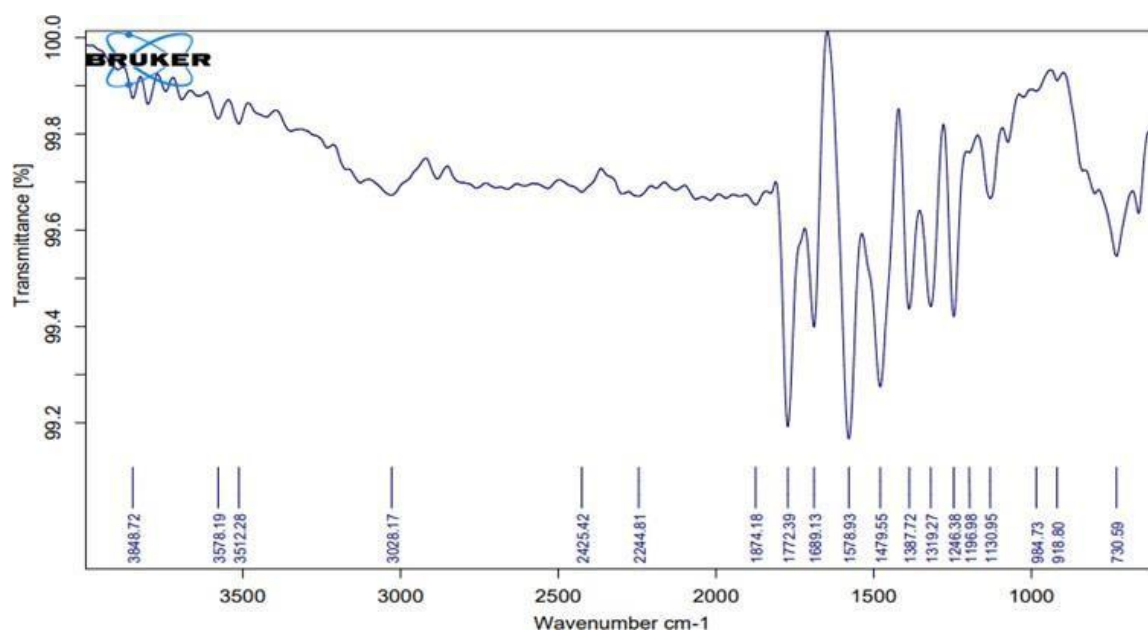


**Figure 5.2: FTIR graph of ampicillin**

The spectra of ampicillin trihydrate showed the expected principal peak at  $1689.13\text{ cm}^{-1}$ , which corresponding to  $C=O$  stretching vibration. Another peak at  $1772.39\text{ cm}^{-1}$  corresponding to  $C=O$  stretching of the  $\beta$ -lactam ring. Other characteristic peaks at  $3028.17\text{ cm}^{-1}$  and  $3512.8\text{ cm}^{-1}$  corresponding to O-H stretching from primary amines and N-H bending vibration respectively. These peaks confirm the presence of essential structural components of ampicillin. The comparison of observed and reported peaks of characteristics functional groups present in ampicillin trihydrate are tabulated in Table 5.3.

**Table 5.3. Characteristic peak of ampicillin trihydrate in FTIR**

Observed peak( $cm^{-1}$ )	Reported peak( $cm^{-1}$ )	Functional group	Expected compound
1689.13	1700-1600	$C=O$ stretching	Amide group
3512.80	3500-2280	N-H stretching	Amine group
3028.17	3060-3040	O-H stretching	Alcohol group

1772.39	1750-1600	C=O bending	$\beta$ -lactam ring
---------	-----------	-------------	----------------------

### Spectroscopic Studies

- Absorption Maxima( $\lambda_{max}$ )**

Ampicillin trihydrate solution (10 $\mu$ g/ml) in water was taken in Cuvette and scanned in the range of 200-400nm on a UV- Spectrophotometer (Shimadzu, Japan) against respective blanks. UV spectra of ampicillin trihydrate are shown in Figure 5.5.

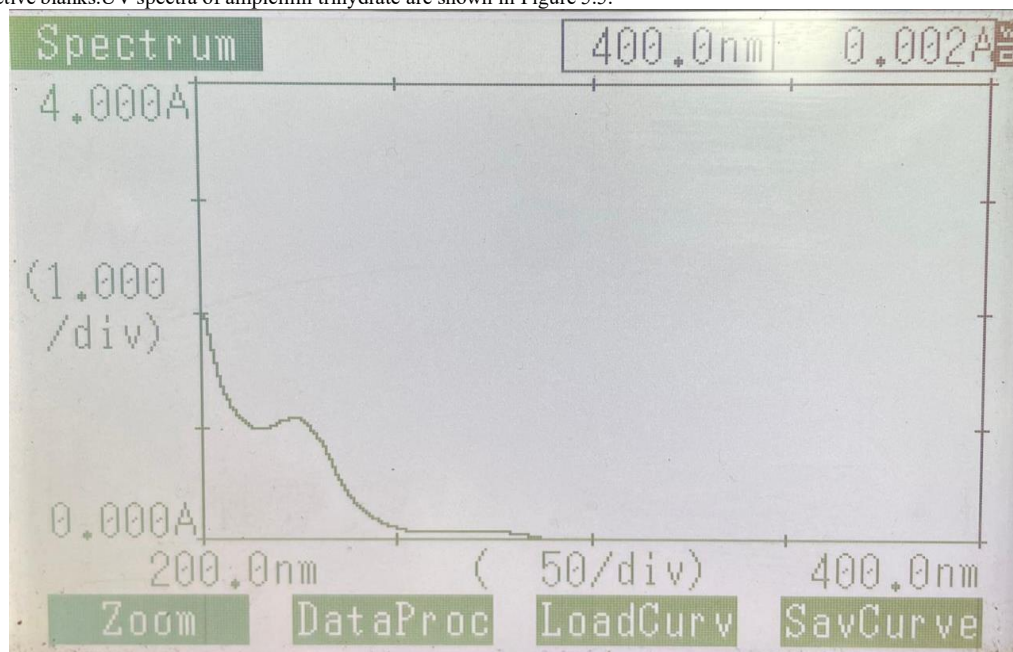


Figure 5.5: UV Spectra of ampicillin

- Preparation of Calibration Curve of ampicillin trihydrate in water**

The calibration curve of ampicillin trihydrate in water depicted in Figure 5.6. The calibration equation for straight line was observed to be  $Y = 0.0279X - 0.0131$  with correlation coefficient( $R^2$ ) of **0.9983** which was used to calculate concentration of samples for analytical purpose (Patel et al., 2012).

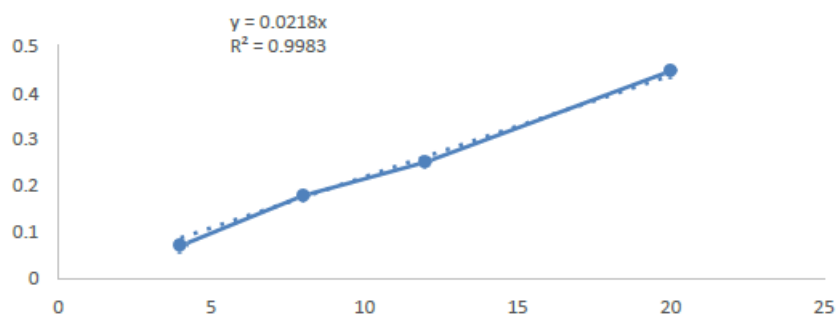


Figure 5.6: Calibration curve of ampicillin trihydrate in water in the range 2.5-20  $\mu$ g/ml

### Selection of *orodispersible* polymers for the final formulation

Out of the seven formulations, F2, F4, F6, and F8 were unable to fabricate nanofibers due to the inappropriate viscosity of the polymeric dispersions. The viscosity of the polymer solution must be within a specific range for successful nanofiber formation. The low-viscosity polymeric dispersions were unable to form fibers and instead produced droplets (a phenomenon called electrospraying). In contrast, the high-viscosity polymeric dispersions could not be poured or run through the syringe during the electrospinning process, as mentioned in Table 5.7. From the other four formulations only F3 formulation was formed fiber with high mechanical strength as compared to the other three formulations. Therefore, PVP K90 was the selected polymer for the fabrication of *orodispersible* nanofibers.

**Table 5.7: Screening of polymers for the final formulation**

S.No	Polymer A	Conc. A	Polymer B	Conc. B	Solvent	Excipients	Observation
F1	Sodium Alginate	2.5%	PVA	10%	Water	-	No fibers formed because of low viscosity
F2	PVA	5%	PVA K30	5%	Water	-	No fibers formed
F3	PVP K90	15%	-	-	Ethanol	2% Citric acid	Fiber formed with good mechanical strength
F4	PVP K90	20%	CMC	1% In water	Ethanol water	-	No fibers formed because CMC was precipitated
F5	PVA	10%	PVP K90	20%	Water	66% sucrose	Mechanical strength was good but fibers were too sticky and were difficult to peel off possibly because of sucrose
F6	PVA	10%	PVPK90	10%	Water	66% sucrose+0.9%	No fibers formed

						NaCl	because of high viscosity of the dispersion
F7	PVA	7%	PVP K90	7%	Water	0.9% NaCl	Fibers formed with poor mechanical strength
F8	PVP K30	20%	-	-	-	2% Citric acid	No fibers formed

**Characterization of Fabricated Electrospun Nanofiber and polymeric dispersion****Visual Inspection of Physical Appearance**

The fabricated nanofibers were inspected visually for its physical appearance and uniformity. The observations are depicted in the table 5.8 and figure 5.7.

**Table 5.8: Physical characteristics of nanofibers**

Parameter	Observation
Physical appearance	A yellowish and opaque nanofiber film was prepared

<b>Uniformity</b>	Nanofiber film was uniform in all directions
<b>Texture</b>	Soft and flexible

#### Thickness of the fiber mat

Fabricated orodispersible nanofiber obtained from 3 different batches were cut into  $2 \times 2 \text{ cm}^2$  area and observed to have uniformity of mass with an average weight of  $38.5 \pm 3.12 \text{ mg}$ . The average thickness of nanofibers sheets was found to be  $0.44 \pm 0.012 \text{ mm}$ . This is entirely appropriate for an oral fast-dissolving film, and can be adjusted very easily by varying the collection time (i.e., the volume of solution processed).

#### Folding endurance

Folding endurance of the prepared nanofiber film was measured by folding the film over 240 times, and there were no cracks in the films. Hence it was considered as the end point and it was found that the folding endurance of the prepared orodispersible film fell between 244 to 255. It concluded that the prepared films possessed excellent film properties and have greater folding endurance (Conte et al., 2020; Mirzaeei et al., 2021).

#### pH of the fiber solution

Solutions prepared by dissolving a  $2 \times 2 \text{ cm}^2$  section of the fiber mats in 10 mL deionized water were found to have pH values lying in the range 6.7–7.2. Acidic or alkaline pHs may cause damage to the oral mucosa, and so the pH of the dissolved oral fast dissolving film should be close to the neutral pH of the mucosa. Mucosal pH values have been found to vary between 6.28 (buccal mucosa) and 7.34 (palate). The materials fabricated here hence give solutions with pHs close to those observed for the oral mucosa, and can be expected not to cause mucosal damage upon administration.

#### Morphology

The SEM images of ampicillin trihydrate loaded orodispersible nanofiber mats are illustrated in fig 5.9. The SEM data showed that the composite fibers were cylindrical in shape, with smooth surfaces and no secondary particles visible. No bead-on-string morphology can be observed. This indicates that the drug is encapsulated homogeneously in the PVP fiber matrices. The fabricated fibers are oriented in a random manner. The diameters of the ampicillin trihydrate acetate loaded fiber were in the range of  $170 \pm 0.3 \text{ nm}$  to  $476 \pm 0.3 \text{ nm}$ .

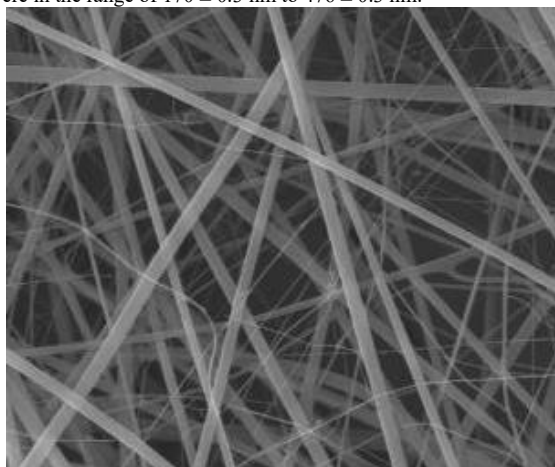


**Figure 5.9: Scanning electron microscopy (SEM) micrographs of the nanofibers produced using polymeric solution of PVP K90 ,citric acid and containing ampicillin.**

#### 5.3.8 Fourier Transform Infrared (FTIR) Spectroscopy of Developed Nanofibers

IR spectra of blank and ampicillin trihydrate loaded orodispersible nanofibers are illustrated in figure 5.10. The observed characteristic peaks in blank and drug loaded fibers were found to be concordant with functional groups. Thus, it was led to the inference that there was no interaction, between drug and polymers in the drug-loaded nanofiber mats.

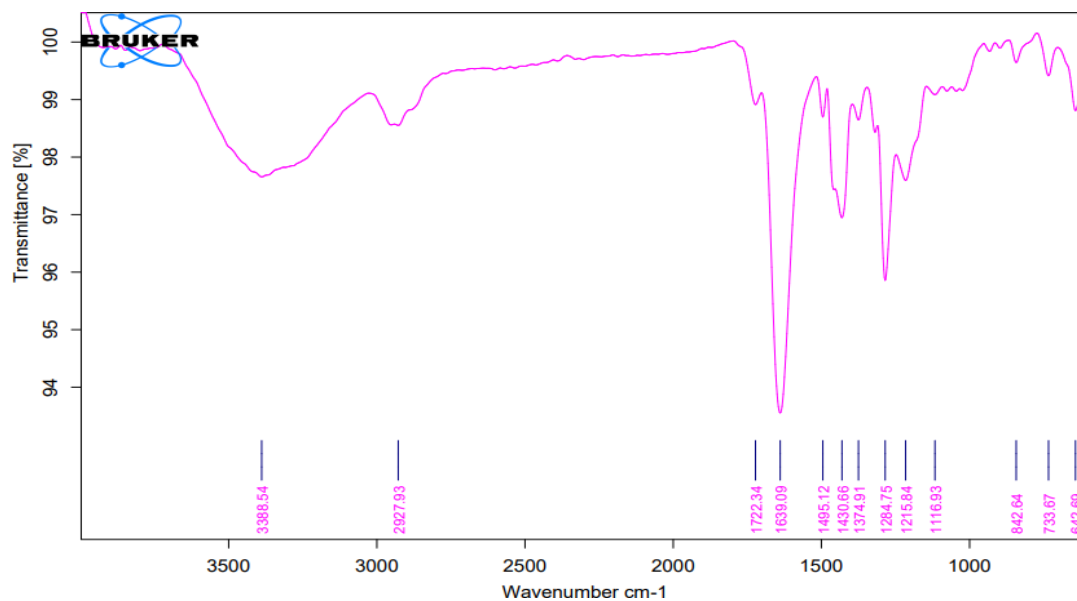


Figure 5.10: FTIR spectra of ampicillin trihydrate loaded nanofiber mat

#### Tensile Strength

A nanofiber with dimensions of 2 cm length and 2 cm width was placed in a vertical position along the y-axis of the Texture analyzer with the help of clamps. After placing the nanofiber, the test was performed to determine the force required to break down the nanofiber and provide data on its mechanical property. According to the graph 5.12 and mentioned parameters in the table 5.9 it showed that the nanofiber possesses enough flexibility and also have good tensile strength. The recorded rib seal strength to break down the drug-loaded orodispersible nanofiber was found to be 2.155 N/mm (Molnar et al., 2012).

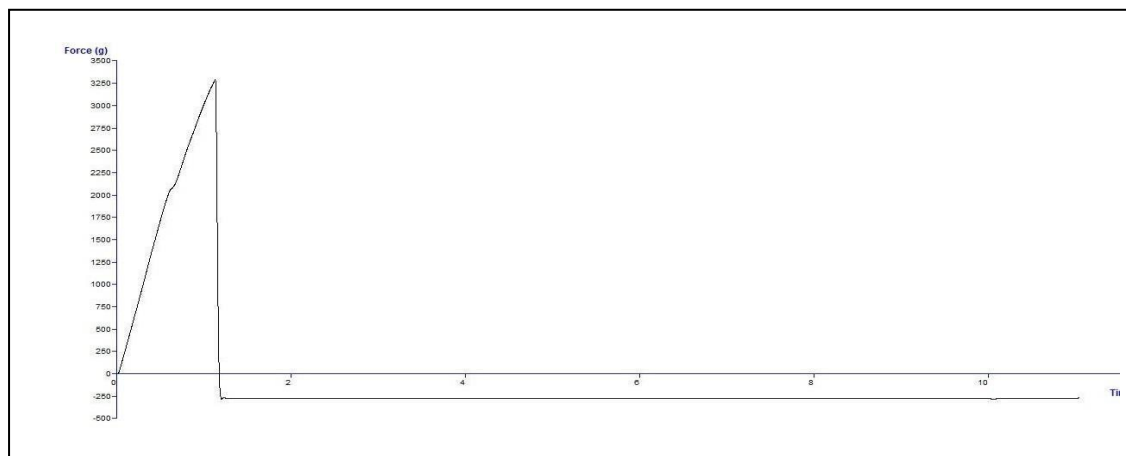


Figure 5.12: Rib seal strength v/s time curve and assembly of prepared nanofibers for tensile strength measurement

Table 5.9: Texture analysis settings and parameters

Parameters	Limits
Pre-Test Speed	1.00 mm/sec
Test Speed:	1.50 mm/sec
Post Test Speed	10.00 mm/sec
Target Mode	Distance

T.A. Variable No.	5: 0.0 g
Distance	32.000 mm
Strain	10.0 %
Trigger Type	Auto (Force)
Trigger Force	5.0 g

### Rheology of drug loaded polymeric dispersion

Rheology is the study of how solution flow under the influence of applied forces. The rheological behavior of polymeric dispersion used in the electrospinning method is a critical parameter for fabrication. There must has a certain range of viscosity of the prepared solution. If the viscosity of the polymeric dispersion is low then there are higher chances for the unsuccessful electrospinning and if the viscosity is too high then it may choke the needle and again fail the electrospinning process. Therefore, drug, PVP K90 and citric acid were combined in such concentration so that they can flow and making electrospinning successful. The obtained viscosity of the polymeric dispersion was found to 441.48 mPa.s as depicted in the figure 5.13. Also, from the shear stress  $\tau$  vs shear rate curve it concluded that the prepared polymeric solution behaved as Non-Newtonian fluid with no clear shear thickening or thinning trend (Holmberg et al., 2021).

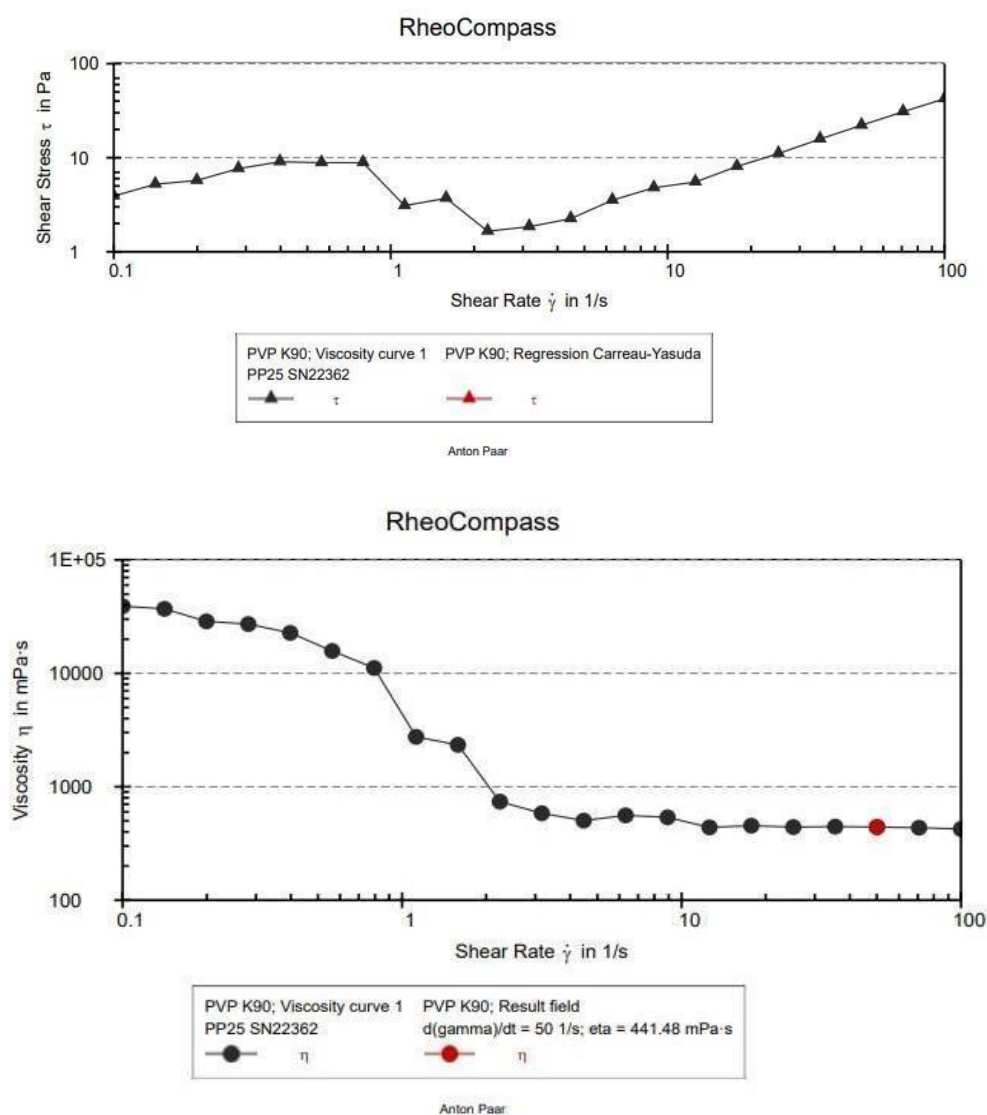


Figure 5.13: Results of rheological evaluation of polymeric dispersion

### Disintegration

The ampicillin trihydrate loaded fiber mats were found to be wetted and to disintegrate very rapidly in simulated saliva. The process was recorded using a standard video camera. fiber mat appeared to disintegrate within <1min when recorded using the standard camera. disintegration time obtained are exceptionally rapid, and eminently suitable for the preparation of oral fast- dissolving film.

### Dissolution studies

The rapid dissolution observed with the ampicillin trihydrate loaded fiber mats can be attributed to the amorphous physical state of the APIs in the formulations, the high surface area and high porosity of the of the drug loaded fibers, and the exceptional hydrophilicity of PVP complete drug was released within <400 seconds.

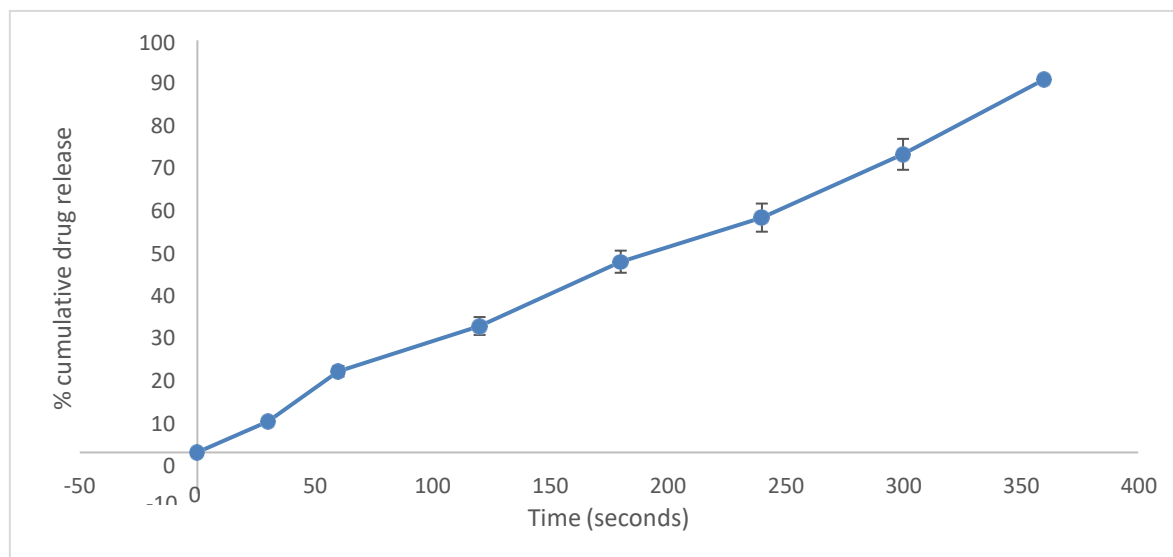


Figure 5.15: *In vitro* dissolution profile

The *in vitro* drug release graph illustrates the release profile of an orodispersible nanofibrous film. Initially, there is a slight lag in drug release during the first 50 seconds, indicating that the film requires a brief period to begin dispersing and releasing the drug. After this, a controlled and gradual release of the drug occurs, with a steady increase in release rate between 50 and 200 seconds. The release profile becomes more linear towards the latter part of the experiment, reaching around 90% cumulative release by 350 seconds. The minimal variability indicated by the error bars suggests a consistent release behaviour across samples. This release pattern highlights the effectiveness of the nanofibrous film in providing a immediate release after rapid dispersion in the initial phase, ideal for orodispersible formulations and the complete drug was released within 400 seconds.

### Drug loading and Entrapment Efficacy

The drug loading was calculated in the prepared orodispersible nanofibers. The obtained result indicated that ampicillin trihydrate loading was  $1.27 \pm 0.57$  % w/w in electrospun nanofibers. Additionally optimizing the drug loading efficiency is essential to develop effective drug delivery system (Pardo-Figueroa et al., 2022), and the entrapment efficiency of for the Ampicillin trihydrate-loaded films was found to be 60%. This indicates that a significant proportion of the drug was successfully entrapped within the nanofibrous matrix.

### 5.3.13 Weight variation

The average weight of the films was found to be 5.89g, with a standard deviation of 0.21g, indicating consistent film thickness and drug loading.

## Summary and conclusion

Local throat pathologies, such as pharyngitis, tonsillitis, and laryngitis, are common inflammatory conditions typically caused by bacterial infections, leading to symptoms such as pain, irritation, and difficulty swallowing. Conventional treatment for these conditions often involves systemic administration of oral antibiotics, which may require prolonged periods to achieve effective drug concentrations at the site of infection. This delay in drug action can result in slower relief from symptoms, while systemic absorption increases the risk of side effects and contributes to the development of antibiotic resistance. In recent years, nanofibrous drug delivery systems have emerged as an innovative alternative to conventional oral medications. Nanofibers produced through electrospinning offer several significant advantages. Due to their high surface area-to-volume ratio, nanofibers allow for rapid disintegration and quick drug release, facilitating localized delivery directly to the affected area in the throat. This not only enhances the bioavailability of the drug but also reduces the need for higher systemic doses, minimizing adverse effects and improving patient compliance. Moreover, the use of nanofibers ensures controlled drug release, which can improve therapeutic outcomes by maintaining effective concentrations of the drug at the infection site for a longer period. The aim of this study was to fabricate and evaluate a nanofibrous oro- dispersible film loaded with Ampicillin

trihydrate, specifically designed for the treatment of throat pathologies. The film was developed using polyvinylpyrrolidone (PVP) K90 as the polymer matrix, while citric acid was incorporated to promote salivation and aid in the rapid disintegration of the film upon contact with saliva and Ethanol was employed as the primary solvent due to its ability to dissolve both the polymer and drug efficiently while also being volatile enough to evaporate during fiber formation, ensuring a dry, stable nanofibrous structure. The electrospinning process was employed to create the nanofibrous structure, with the goal of achieving immediate drug release and improved therapeutic efficacy for throat infections. To evaluate the pharmaceutical performance of the developed films, various parameters were examined. Preformulation studies including solubility of ampicillin trihydrate was determined using various solvents such as methanol, ethanol, water, DMF and DMSO. The partition coefficient of ampicillin trihydrate acetate was found to be -0.24. Before the preparation of nanofibers, the rheological study of polymeric dispersion showed Non Newtonian flow behavior with obtained viscosity of 441.48 mPa.s. Prepared nanofibers showed consistency for weight, thickness, structure and the surface pH of the nanofiber was 7.4 which is in the range of pH of saliva (pH 5.6-7.9). The diameter of the nanofibers was in the range of  $170 \pm 0.3$  nm to  $476 \pm 0.3$  nm. Our electrospun nanofiber displayed disintegration within <1min which is essential for an oro-dispersible formulation. The tensile strength of the prepared nanofibers were found to 2.155N/mm. The drug loading and dissolution studies were carried out to quantify the antibiotic content and assess the release profile of Ampicillin trihydrate from the nanofibers.

## REFERENCES:

1. Al-Shaeli, M., S. Benkhaya, R. A. Al-Juboori, I. Koyuncu and V. Vatanpour (2024). "pH-responsive membranes: Mechanisms, fabrications, and applications." *Sci Total Environ* **946**: 173865.
2. Alshahrani, S. M., N. Thotakura, S. Sharma, S. S. Qadir, N. Chaurawal, S. Sharma, D. Chitkara and K. Raza (2023). "Influence of Nanocarrier Type on the Drug Delivery Aspects of Docetaxel: Empirical Evidences." *Journal of Pharmaceutical Innovation* **18**(2): 641-652.
3. Azari, A., A. Golchin, M. Mahmoodinia Maymand, F. Mansouri and A. Ardeshiryajimi (2022). "Electrospun Polycaprolactone Nanofibers: Current Research and Applications in Biomedical Application." *Adv Pharm Bull* **12**(4): 658-672.
4. Conte, F., N. Cellini, O. De Rosa, A. Caputo, S. Malloggi, A. Coppola, B. Albinni, M. Cerasuolo, F. Giganti, R. Marcone and G. Ficca (2020). "Relationships between Dream and Previous Wake Emotions Assessed through the Italian Modified Differential Emotions Scale." *Brain Sci* **10**(10).
5. Dabadghao, S. S. and B. Vaziri (2022). "The predictive power of popular sports ranking methods in the NFL, NBA, and NHL." *Operational Research* **22**(3): 2767-2783.
6. Edmans, J. G., K. H. Clitherow, C. Murdoch, P. V. Hatton, S. G. Spain and H. E. Colley (2020). "Mucoadhesive Electrospun Fibre-Based Technologies for Oral Medicine." *Pharmaceutics* **12**(6).
7. Fan, J., S. Yu, K. Qi, C. Liu, L. Zhang, H. Zhang, X. Cui and W. Zheng (2018). "Synthesis of ultrathin wrinkle-free PdCu alloy nanosheets for modulating d-band electrons for efficient methanol oxidation." *Journal of Materials Chemistry A* **6**(18): 8531-8536.
8. García-León, M., J. M. Pérez-Mármol, R. Gonzalez-Pérez, M. D. C. García-Ríos and M. I. Peralta-Ramírez (2019). "Relationship between resilience and stress: Perceived stress, stressful life events, HPA axis response during a stressful task and hair cortisol." *Physiol Behav* **202**: 87-93.
9. Hoseyni, S. Z., S. M. Jafari, H. S. Tabarestani, M. R. Ghorbani, E. Assadpour and M. J. F. H. Sabaghi (2021). "Release of catechin from Azivash gum-polyvinyl alcohol electrospun nanofibers in simulated food and digestion media." **112**: 106366.
10. Hughes, K., M. A. Bellis, K. A. Hardcastle, D. Sethi, A. Butchart, C. Mikton, L. Jones and M. P. Dunne (2017). "The effect of multiple adverse childhood experiences on health: a systematic review and meta-analysis." *Lancet Public Health* **2**(8): e356-e366.
11. Jayaraman, K., M. Kotaki, Y. Zhang, X. Mo and S. Ramakrishna (2004). "Recent advances in polymer nanofibers." *J Nanosci Nanotechnol* **4**(1-2): 52-65.
12. Kato, H., Y. Yamagishi, M. Hagihara, J. Hirai, N. Asai, Y. Shibata, T. Iwamoto and H. Mikamo (2022). "Systematic review and meta-analysis for impacts of oral antibiotic treatment on pregnancy outcomes in chronic endometritis patients." *J Infect Chemother* **28**(5): 610-615.
13. Kida, S. (2023). "Interaction between reconsolidation and extinction of fear memory." *Brain Res Bull* **195**: 141-144.
14. Kumar, L., S. Verma, K. Joshi, P. Utreja and S. Sharma (2021). "Nanofiber as a novel vehicle for transdermal delivery of therapeutic agents: challenges and opportunities." *Future Journal of Pharmaceutical Sciences* **7**(1): 175.
15. Li, Y., S. Xiao, Y. Luo, S. Tian, J. Tang, X. Zhang and J. Xiong (2022). "Advances in electrospun nanofibers for triboelectric nanogenerators." *Nano Energy* **104**: 107884.
16. Lohan, S., S. Sharma and R. M. Rayasa (2013). "Formulation and Evaluation of Solid Lipid Nanoparticles of Quetiapine Fumarate and Quetiapine Hemifumarate for Brain Delivery in Rat Model." *Pharmaceutical Nanotechnology* **1**(3): 239-247.
17. Mirzaei, R., A. Afaghi, S. Babakhani, M. R. Sohrabi, S. R. Hosseini-Fard, K. Babolhavaeji, S. Khani Ali Akbari, R. Yousefimashouf and S. Karampoor (2021). "Role of microbiota-derived short-chain fatty acids in cancer development and prevention." *Biomed Pharmacother* **139**: 111619.
18. Mishra, A., V. R. Sinha, S. Sharma, A. T. Mathew, R. Kumar and A. K. Yadav "A comprehensive compatibility study of ganciclovir with some common excipients." *American Journal of Biopharmacy and Pharmaceutical Sciences* **3**: 2.
19. Molnar, M. Z., R. Mehrotra, U. Duong, S. Bunnapradist, L. R. Lukowsky, M. Krishnan, C. P. Kovesdy and K. Kalantar-Zadeh (2012). "Dialysis modality and outcomes in kidney transplant recipients." *Clin J Am Soc Nephrol* **7**(2): 332-341.
20. Nadaf, A., A. Gupta, N. Hasan, Fauziya, S. Ahmad, P. Kesharwani and F. J. Ahmad (2022). "Recent update on electrospinning and electrospun nanofibers: current trends and their applications." *RSC Adv* **12**(37): 23808-23828.

21. Ramenskaya, G. V., V. S. Shlykov and O. A. Dekhanova (2008). "Comparative in vitro dissolution testing of indapamide prolonged-release tablets." *Pharmaceutical Chemistry Journal* **42**(12): 726-729.
22. Savjani, K. T., A. K. Gajjar and J. K. Savjani (2012). "Drug solubility: importance and enhancement techniques." *ISRN Pharm* **2012**: 195727.
23. Sension, R. J., T. Chung, P. Dewan, Jr., T. P. McClain, R. M. Lamb and J. E. Penner-Hahn (2022). "Time-resolved spectroscopy: Advances in understanding the electronic structure and dynamics of cobalamins." *Methods Enzymol* **669**: 303-331.
24. Sharma, S., S. Lohan and R. S. Murthy (2014). "Formulation and characterization of intranasal mucoadhesive nanoparticulates and thermo-reversible gel of levodopa for brain delivery." *Drug Dev Ind Pharm* **40**(7): 869-878.
25. Sharma, S. and V. R. Sinha (2020). "In vitro and in vivo amelioration of colitis using targeted delivery system of cyclosporine a in New Zealand rabbits." *Drug Development and Industrial Pharmacy* **46**(10): 1726-1733.
26. Tort, S. and F. Acartürk (2016). "Preparation and characterization of electrospun nanofibers containing glutamine." *Carbohydrate Polymers* **152**: 802-814.
27. Voronova, A., C. Prieto, M. Pardo-Figuerez, J. M. Lagaron, A. Sanyal, B. Demir, T. Hubert, V. Plaisance, V. Pawlowski, S. Vignoud-Despond, A. Barras, A. Abderrahmani, R. Boukherroub and S. Szunerits (2022). "Photothermal Activatable Mucoadhesive Fiber Mats for On-Demand Delivery of Insulin via Buccal and Corneal Mucosa." *ACS Appl Bio Mater* **5**(2): 771-778.
28. Walczak, J., D. Iwaszkiewicz-Grześ and G. Cholewiński (2024). "Approaches Towards Better Immunosuppressive Agents." *Curr Top Med Chem* **24**(14): 1230-1263.
29. Yang, J., H. Yao, Y. Guo, B. Yang and J. Shi (2022). "Enhancing Tumor Catalytic Therapy by Co-Catalysis." *Angew Chem Int Ed Engl* **61**(17): e202200480.
30. Yoon, K., B. S. Hsiao and B. Chu (2008). "Functional nanofibers for environmental applications." *Journal of Materials Chemistry* **18**(44): 5326-5334.
31. Zaarour, B., L. Zhu and X. Jin (2020). "Direct generation of electrospun branched nanofibers for energy harvesting." *Polymers for Advanced Technologies* **31**(11): 2659-2666.